ELSEVIER

Journal of Alloys and Compounds 356–357 (2003) 120–127

Journal of ALLOYS AND COMPOUNDS

www.elsevier.com/locate/jallcom

Crystal structures and thermal properties of titanium carbo-deuterides as prepared by combustion synthesis

G. Renaudin[a], K. Yvon[a,*], S.K. Dolukhanyan[b], N.N. Aghajanyan[b], V.Sh. Shekhtman[c]

[a]*Laboratory of Crystallography, University of Geneva, 24 quai Ernest Ansermet, 1211 Geneva, Switzerland*
[b]*Institute of Chemical Physics of Armenian National Academy of Sciences, 375044 Yerevan, Armenia*
[c]*Institute of Solid State Physics of Russian Academy of Sciences, 142432 Chernogolovka, Russia*

Received 26 July 2002; accepted 15 November 2002

Abstract

Titanium carbo-deuterides of various compositions have been prepared by thermal radiation and cold syntheses, and by self-propagating high-temperature synthesis. While the former methods favored the formation of a cubic structure of composition $TiC_{0.48(1)}D_{0.60(2)}$ ($Fm\bar{3}m$, $a=4.30963(3)$ Å) the latter yielded a trigonal structure of composition $TiC_{0.50(-)}D_{0.707(4)}$ ($P\bar{3}m1$, $a=3.08208(2)$, $c=5.04052(6)$ Å). Differential thermal analysis and thermogravimetry data suggest the cubic structure to be thermally less stable (desorption onset temperature 823 K) than the trigonal structure (1093 K). Joint Rietveld structure refinements based on neutron and X-ray powder diffraction data show that carbon occupies octahedral interstices in the *f.c.c.* and *h.c.p.* metal atom networks of the cubic and trigonal phase, respectively, while deuterium occupies both octahedral and tetrahedral interstices in the cubic but tetrahedral interstices only in the trigonal phase. The different thermal stability of the compounds is attributed to these structural differences.

Keywords: Hydrogen storage materials; Interstitial alloys; Gas–solid reaction; X-ray and neutron diffraction; Thermal analysis

1. Introduction

Hydrogen reacts with transition metal carbides to form so-called carbo-hydrides. Representative examples occur in systems based on titanium [1–6], zirconium [3–5,7–10], hafnium [2,3,5], vanadium [9,10], niobium [5] and others. The compounds crystallise mostly with face-centred cubic (*f.c.c.*) and/or hexagonal close-packed (*h.c.p.*) metal atom arrangements in which carbon and hydrogen atoms occupy octahedral and/or tetrahedral interstices, respectively. In spite of their interest as potential hydrogen storage materials only few carbo-hydride systems have been studied in detail with respect to structural and thermal properties. The Ti–C–H system, for example, contains two carbo-hydride phases that crystallise with cubic and trigonal symmetry [1–6]. While the cubic phase has been investigated by neutron diffraction [6] no structure refinement has been performed and no atomic parameters were reported for the trigonal phase. Thermal stability data are also not available. In this paper we present the first structure refinements of, and thermal stability data for the Ti–C–H system. The samples investigated were obtained by combustion synthesis [11–13]. This method is of particular interest in the context of hydrogen storage materials because it is capable of yielding large quantities of materials at a relatively low cost. Consequently, the structural and thermal properties reported in this paper refer to relatively extreme conditions of synthesis.

2. Experimental

2.1. Sample preparation

Two sorts of samples were prepared by combustion of binary titanium carbide of nominal composition $TiC_{0.4}$ in a deuterium atmosphere. One sample was prepared by the so-called self-propagating high-temperature synthesis (SHS) method [11]. Compressed tablets (20 mm diameter and 35 mm high) of a powder mixture of nominal composition Ti + 0.4C were placed into a hermetic reactor at a constant deuterium pressure of 3 bar and ignited

*Corresponding author. Tel.: +41-22-702-6231; fax: +41-22-702-6864.
E-mail address: klaus.yvon@cryst.unige.ch (K. Yvon).

0925-8388/03/$ – see front matter
doi:10.1016/S0925-8388(03)00107-5

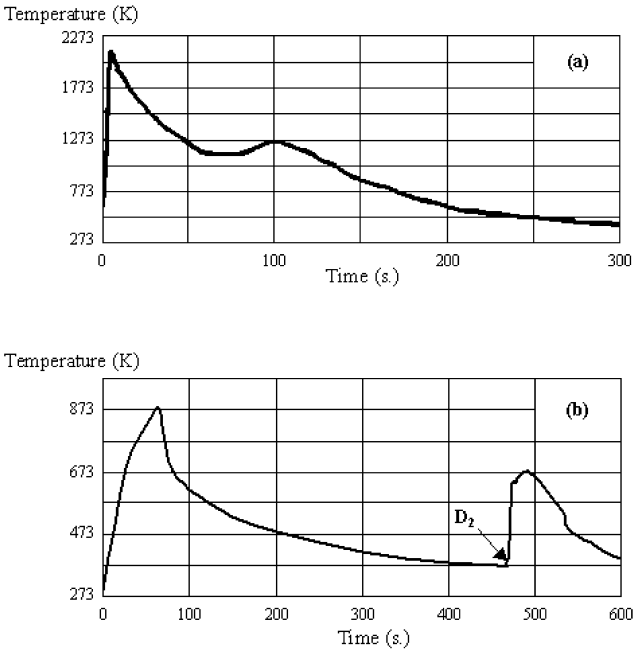

Fig. 1. Sample temperature for titanium carbo-deuterides as a function of time (s) during the SHS (a) and CS reactions (b). Arrow 'D_2' marks the filling of the thermal radiation chamber with 2 bar of deuterium gas and corresponds to the beginning of the CS process after the TRS process.

locally by heating a tungsten spiral. As shown by the temperature profile in Fig. 1a the reaction temperature reached rapidly a maximum of 2000 K while the velocity of the combustion wave front was ~5 cm s^{-1}. As will be shown below this sample (called SHS sample) contained mainly the trigonal phase of refined composition $TiC_{0.50}D_{0.71}$. Another sample was obtained in the accelerated electron beam as a result of the interaction between binary titanium carbide and deuterium. A tablet (20 mm diameter and 5 mm high) was pressed from titanium carbide of nominal composition $TiC_{0.4}$ as synthesized by the SHS method and placed into an evacuated chamber on a high-current linear electron accelerator LAE-5 where it was irradiated in a focused electronic beam (see Fig. 1 in Ref. [12]). The working parameters of the accelerator were 4 MeV power and 150 μA average current. The collimated electron beam provided an even irradiation over the entire sample volume. The $TiC_{0.4}$ tablet was first irradiated in vacuum at a dose rate of 0.7 Mrad s^{-1} during 70 s, (total dose of 50 Mrad). This procedure resulted in an increase of the sample temperature to 873 K. After 400 s, the electronic beam was switched off and the sample was allowed to cool down to a temperature of about 373 K while the chamber was filled with 2 bar of deuterium gas. The exothermic reaction between the irradiated titanium carbide and deuterium resulted in an increase of the sample temperature to 673 K, the profile of which is shown in Fig. 1b. This reaction has been referred to as 'cold-synthesis' (CS) [12]. As shown below the sample (called CS sample) contained mainly a cubic phase of refined composition $TiC_{0.48}D_{0.60}$.

2.2. Thermal analysis

The thermal stability of the samples was studied by differential thermal analysis (DTA) on a Dichrograph Q-1500 and by thermogravimetry (TG). To prevent oxidation of the sample, the DTA experiments have been conducted under an argon flow at a permanent rate of 20 ml min^{-1}. Experiments have been carried out from room temperature up to 1273 K with a heating rate of 20 K min^{-1}. The thermo-gravimetric (TG) and differential thermal analysis (DTA) data are shown in Fig. 2.

2.3. X-ray and neutron diffraction

X-ray powder diffraction experiments were performed on a Bruker D8 diffractometer (Bragg–Brentano geometry, Cu $K\alpha_1$ radiation) at room temperature. The CS sample was measured in the 2θ range 25–140° during 20 h with a

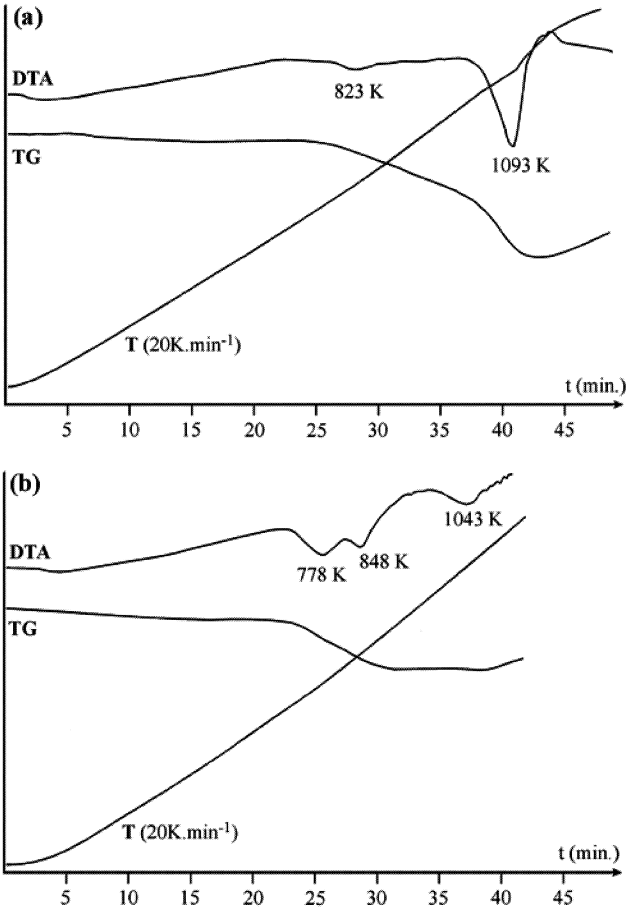

Fig. 2. Differential thermal analysis (DTA) and thermogram (TG) of titanium carbo-deuterides as a function of time (min) for SHS (a) and CS sample (b). Measurements from room temperature to 1273 K at a heating rate of 20 K min^{-1} in an argon flow.

step size of $2\theta = 0.0144°$ and found to consist mainly of the cubic carbo-deuteride phase and of ~10 wt% binary titanium deuteride TiD_2. The SHS sample was measured in the 2θ range 10–137° during 22 h with the same step size and found to contain mainly the trigonal carbo-deuteride phase and minor amounts of cubic titanium carbo-deuteride and titanium deuteride TiD_2 (<10 wt% each). The full widths at half maximum (FWHM) of the TiD_2 reflections in both samples were about four times as large as those observed for the titanium carbo-deuteride phase and thus were modelled in terms a cubic rather than tetragonal lattice symmetry. Neutron powder diffraction experiments were performed on HRPT [14] at SINQ (PSI, Villigen) at room temperature. The samples (~5 g mass) were enclosed in cylindrical vanadium containers of 8 mm inner diameter and measured at a wavelength of $\lambda = 1.196$ Å in the 2θ ranges 3–163° (CS sample) and 5–165° (SHS sample) with a step size of $2\theta = 0.05°$. Transmission factors were calculated ($\mu R = 0.09$) and the data corrected accordingly. The patterns showed the same phases and phase proportions as those found by X-ray diffraction, i.e. the cubic carbo-deuteride and some TiD_2 for the CS sample and the trigonal carbo-deuteride, some cubic titanium carbo-deuteride and some TiD_2 for the SHS sample. The diffraction peaks of the TiD_2 phase were again considerably broadened in both patterns. No superstructure lines were detected for the cubic carbo-deuteride patterns, neither in the X-ray nor in the neutron data indicative for a cell increase due to carbon ordering as found in cubic titanium carbo-hydrides [6] or in cubic zirconium carbo-hydride [2,4]. Likewise, no superstructure lines were detected for the trigonal carbo-deuteride patterns as found in hexagonal yttrium carbo-deuteride [15].

2.4. Structure refinement

Joint Rietveld refinements based on the simultaneous use of the neutron and X-ray data were performed for both samples by the program FullProf.2000 Multi-Pattern [16]. This technique allowed to alleviate the difficulties due to the relatively weak scattering contrast between deuterium and carbon for neutrons (neutron coherent scattering lengths are 6.674 and 6.653 fm for deuterium and carbon, respectively) and the relatively weak scattering power of deuterium for X-rays. For the CS sample the carbon and deuterium atoms were assumed to be distributed at random over the octahedral interstices of the cubic carbo-deuteride (space group $Fm\bar{3}m$, Ti on site 4*a*, C and D on site 4*b*). Preliminary refinements without constraints on the individual occupancy factors showed that the sum of the C and D occupancies of the octahedral interstices did not differ significantly from unity, and that the tetrahedral interstices (site 8*c*) were weakly but significantly occupied by deuterium. During the final refinement the total occupancy of site 4*b* was fixed to unity. The results showed that the octahedral interstices were occupied by 48% of carbon and 52% of deuterium, and the tetrahedral interstices by 4.1(3)% of deuterium, thus yielding a refined overall composition of $TiC_{0.48(1)}D_{0.60(2)}$ ($a = 4.30963(3)$ Å). A Thompson–Cox–Hastings pseudo-Voigt peak-shape function was used for the neutron data, and a pseudo-Voigt function for the X-ray data. In all, 26 parameters were refined: two zero shifts, four scale factors, 11 profile, two cell and seven atomic parameters (five isotropic displacements and two occupancies). A quantitative phase analysis indicated a refined value of 11(2) weight percent of TiD_2 phase (the composition of this phase was fixed at two deuterium per titanium atom as suggested by the cubic cell parameter 4.4316(3) Å [17]). Refinement results are given in Table 1 and interatomic distances in Table 2. Observed and calculated diffraction patterns are shown in Fig. 3.

For the SHS sample the main carbo-deuteride phase was assumed to be isostructural with the trigonal Zr_2CH phase reported previously [4]. The titanium atoms were placed on site 2*d* (1/3,2/3,*z* etc, $z = 0.235$) of space group $P\bar{3}m1$, the carbon atoms on site 1*a* (0,0,0 etc., centre of octahedral interstices) and the deuterium atoms on site 2*d* ($z = 0.61$, centre of tetrahedral interstices). Other possible distributions such as an additional occupancy of site 1*b* (0,0,1/2, etc., 2nd set of octahedral interstices) by carbon and/or deuterium, or of sites 2*d* ($z \sim 0.88$, 2nd set of tetrahedral interstices) by deuterium were checked but found to give no evidence for a significant occupancy of these sites. On the other hand, no indication was found for the possible occurrence of carbon defects on site 1*a*. Thus, during the final refinement cycles the carbon occupancy of site 1*a* was fixed to unity while those in the 2nd sets of interstices were fixed at zero. The results showed that the set of tetrahedral interstices was occupied by 71% of deuterium, yielding the overall composition $TiC_{0.5(-)}D_{0.707(4)}$ ($a = 3.08208(2)$, $c = 5.04052(6)$ Å). A Thompson–Cox–Hastings pseudo-Voigt peak-shape function was used for the neutron data, and a pseudo-Voigt function for the X-rays data. In all, 39 parameters were refined: two zero shifts, six scale factors, 21 profile, four cell and six atomic parameters (two *z* positions, three isotropic displacements and one occupancy). The atomic parameters of the secondary phases (6(2) wt% of cubic $TiC_{0.48}D_{0.60}$ and 5(2) wt% of TiD_2) were fixed at the values refined from the CS sample. Refinement results are also given in Table 1 and interatomic distances are compared with those of the cubic modification in Table 2. Observed and calculated diffraction patterns are shown in Fig. 4.

3. Results and discussion

In spite of their rather extreme conditions of synthesis the present titanium carbo-deuterides show features very similar to those of the carbo-hydrides obtained previously by conventional synthesis. Cubic $TiC_{0.48(1)}D_{0.60(2)}$ is a pseudo-ternary compound that derives by insertion of

Table 1
Joint neutron and X-ray refinement results from CS and SHS samples (e.s.d. values in parentheses)

	Atom	Site	x/a	y/b	z/c	B_{iso} (Å^2)	Occupancy
CS sample							
$TiC_{0.48(1)}D_{0.60(4)}$	Ti	4*a*	0	0	0	0.45(2)	1(−)
*Fm*3*m*, *Z*=4	C_{octa}	4*b*	0.5	0.5	0.5	0.70(7)	0.48(1)*
a=4.30963(3) Å	D_{octa}	4*b*	0.5	0.5	0.5	2.0(1)	0.52(−)*
V=80.042(2) Å^3	D_{tetra}	8*c*	0.25	0.25	0.25	=*B*(D_{octa})	0.041(3)
SHS sample							
$TiC_{0.5}D_{0.707(4)}$	Ti	2*d*	0.3333	0.6667	0.2346(2)	0.11(1)	1(−)
*P*3*m*1, *Z*=2	C_{octa}	1*a*	0	0	0	0.46(1)	1(−)
a=3.08208(2) Å	D_{tetra}	2*d*	0.3333	0.6667	0.6114(3)	0.88(2)	0.707(4)
c=5.04052(6) Å							
c/*a*=1.63543(3)							
V=41.466(1) Å^3							
TiD_2							
*Fm*3*m*, *Z*=4	Ti	4*a*	0	0	0	0.68(9)	1(−)
a=4.4316(3) Å	D_{tetra}	8*c*	0.25	0.25	0.25	1.73(6)	1(−)

Rietveld agreement indices and abundance of secondary phases:
CS sample: global χ^2=7.6. Neutron data (21 *hkl* values): R_{Bragg}=4.7, R_{wp}=9.6 and χ^2=13.2. X-rays data (11 *hkl* values): R_{Bragg}=4.5, R_{wp}=15.3 and χ^2=1.9; TiD_2: ~10 wt%.
SHS sample: global χ^2=3.4. Neutron data (99 *hkl* values): R_{Bragg}=3.5, R_{wp}=7.7, χ^2=4.4. X-ray data (44 *hkl* values): R_{Bragg}=13.4, R_{wp}=18.8, χ^2=1.8; TiD_2 and cubic carbodeuteride phase: <10 wt% each.
* Total occupancy constrained to 1.0.

Table 2
Interatomic distances[a] for cubic and trigonal titanium carbo-deuterides

Cubic $TiC_{0.48(1)}D_{0.60(2)}$		Trigonal $TiC_{0.5(-)}D_{0.707(4)}$	
Bonds	Distance (Å)	Bonds	Distance (Å)
Ti–8 D_{tetra}	1.866	Ti–3 $\square_{tetra}$[b]	1.852
Ti–6 $(C,D)_{octa}$	2.155	Ti–$\square_{tetra}$	1.853
Ti–12 Ti	3.048	Ti–D_{tetra}	1.899
		Ti–3 D_{tetra}	1.941
		Ti–3 C_{octa}	2.137
		Ti–3 $\square_{octa}$[b]	2.226
		Ti–3 Ti	2.960
		Ti–6 Ti	3.082
		Ti–3 Ti	3.213
$(C,D)_{octa}$–8 D_{tetra}	1.866	C_{octa}–6 $\square_{tetra}$	1.902
$(C,D)_{octa}$–6 Ti	2.155	C_{octa}–6 Ti	2.137
		C_{octa}–2 $\square_{octa}$	2.521
		C_{octa}–6 D_{tetra}	2.646
		$\square_{octa}$–6 D_{tetra}	1.866
		D_{tetra}–6 Ti	2.226
		D_{tetra}–2 C_{octa}	2.521
D_{tetra}–4 $(C,D)_{octa}$	1.866	D_{tetra}–$\square_{tetra}$	1.288
D_{tetra}–4 Ti	1.866	D_{tetra}–3 $\square_{octa}$	1.866
D_{tetra}–6 D_{tetra}	2.1550	D_{tetra}–Ti	1.899
		D_{tetra}–3 Ti	1.941
		D_{tetra}–3 D_{tetra}	2.104
		D_{tetra}–3 C_{octa}	2.646
		$\square_{tetra}$–1 D_{tetra}	1.288
		D_{tetra}–3 Ti	1.852
		D_{tetra}–Ti	1.853
		D_{tetra}–3 C_{octa}	1.902

[a] All e.s.d. values smaller than 0.002.
[b] $\square_{tetra}$ and $\square_{octa}$: centres of empty tetrahedral (1/3,2/3,0.867; etc) and octahedral (0,0,1/2; etc) sites.

deuterium into the structure of the carbon deficient binary carbide TiC_{1-x}. Its *f.c.c.* metal atom substructure (*a*=4.31 Å) is slightly expanded compared to deuterium free $TiC_{0.5}$ (*a*/2=4.30 Å [18]) but somewhat compressed compared to the more carbon rich and hydrogen poor carbo-hydride series $TiC_{0.55}H_{0.17}$–$TiC_{0.7}H_{0.2}$ (*a*/2=4.31–4.33 Å, ordered superstructure [6]) or the carbon free binary hydride δ-TiH_2 (*a*=4.46 Å [11]). Trigonal $TiC_{0.5(-)}D_{0.707(4)}$ is a ternary compound that is stabilised by hydrogen. Its *h.c.p.* metal atom substructure (*c*/*a*=1.635) is analogous to elemental α-Ti (*c*/*a*=1.587) and corresponds closely to that of binary subcarbides such as V_2C (*c*/*a*=1.584). Interestingly, despite their almost identical compositions and metal interstices both carbo-deuteride structures show rather different deuterium atom distributions. In the cubic structure the octahedral interstices are fully occupied by a mixture of carbon and deuterium and the tetrahedral interstices are partially occupied (~4%) by deuterium. In the trigonal structure one subset of the octahedral interstices are fully occupied by carbon (C_{octa}) and one subset of the tetrahedral interstices are partially occupied by deuterium (D_{tetra}) while the other subsets ($\square_{tetra}$ and $\square_{octa}$) are empty. These differences are presumably due to the different relative arrangements of the octahedral and tetrahedral interstices in *f.c.c.* and *h.c.p.* metal arrangements and their effect on the non-metal interactions. In the *f.c.c.* arrangement the octahedral and tetrahedral interstices are relatively close to each other (C_{octa}–D_{tetra}=1.87 Å in $TiC_{0.48(1)}D_{0.60(2)}$, see Table 2 and Fig. 5), i.e. repulsive interactions between neighbouring carbon and deuterium atoms render their simultaneous occupancy difficult, at least at high carbon contents. At relatively low carbon contents some of the tetrahedral sites can be occupied by

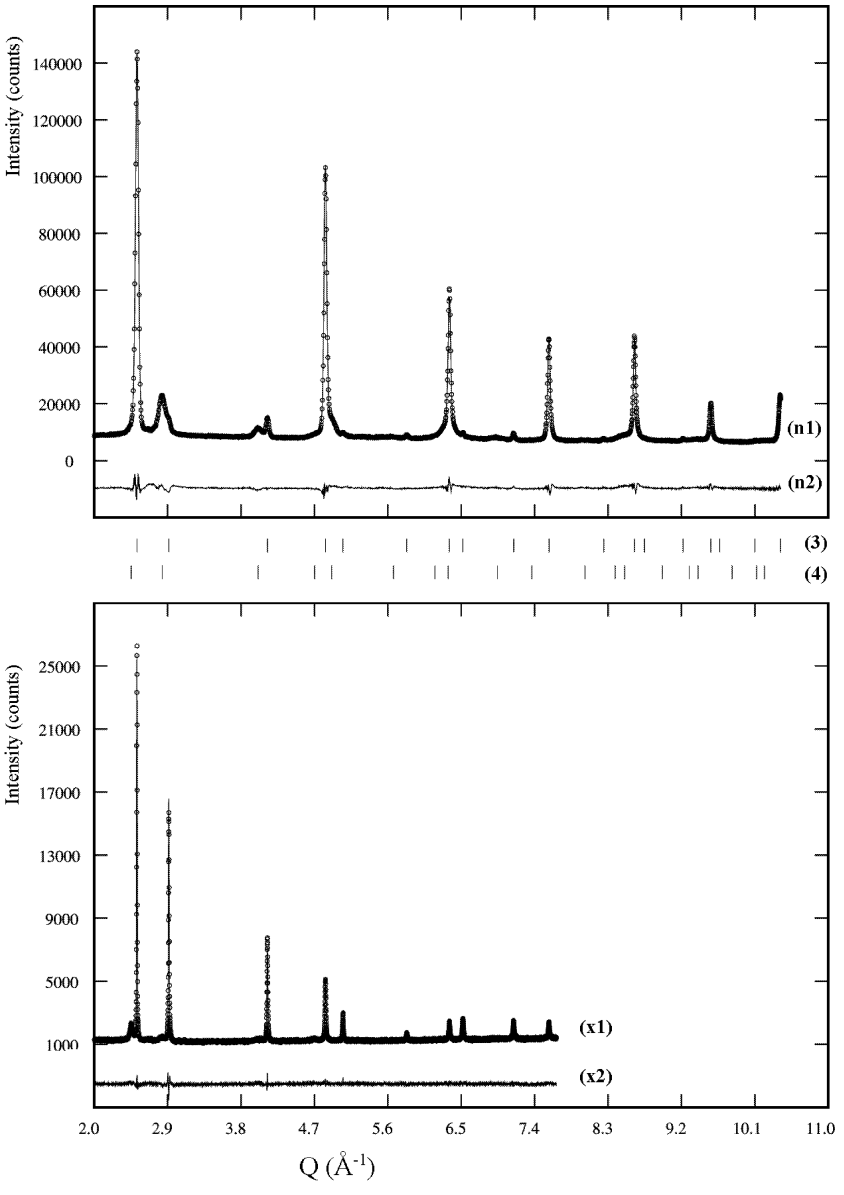

Fig. 3. Observed and calculated (n1), and difference (n2) neutron (top) and X-ray (bottom) powder diffraction patterns for CS sample, and Bragg positions for cubic titanium carbo-deuteride (3) and TiD_2 (4).

deuterium provided their nearest neighbour octahedral sites are not occupied by carbon. For the presently studied carbo-deuteride (Ti/C = 0.48) this situation happens with an estimated probability of about 7% (or less if empty second nearest neighbours tetrahedral sites are considered), which is not far from the experimentally observed occupancy of 4% for the tetrahedral sites.

In the *h.c.p.* arrangement the octahedral and tetrahedral interstices are relatively distant from each other (C_{octa}–D_{tetra} = 2.65 Å in $TiC_{0.5(-)}D_{0.707(4)}$), i.e. repulsive interactions between carbon and deuterium atoms tend to have a smaller influence. However, such interactions also play a role in this structure as can be seen from the non metal-to-metal distances and the sequence of empty and filled interstices along the trigonal axis. As shown in Fig. 5 the carbon atoms in the octahedral holes are ordered such as to avoid close contacts with other carbon atoms ($\square_{octa}$–C_{octa} = 2.52 Å) or with deuterium atoms ($\square_{octa}$–D_{tetra} = 1.87 Å), and the deuterium atoms are partially ordered such as to avoid close contacts with both deuterium ($\square_{tetra}$–D_{tetra} = 1.29 Å) and carbon atoms ($\square_{tetra}$–C_{octa} = 1.90 Å). Furthermore, the occupied octahedral holes are significantly smaller than the empty ones (C_{octa}–Ti = 2.14 Å versus $\square_{octa}$–Ti = 2.23 Å), while the occupied tetrahedral holes are bigger than the empty ones ($\square_{tetra}$–Ti ~1.85 Å, versus D_{tetra}–Ti = 1.90–1.94 Å). This leads to a sequence of carbon and hydrogen containing structure slabs of various thickness along the trigonal axis suggesting partially ionic and covalent bonding components. Similar effects are not apparent in the cubic phase because

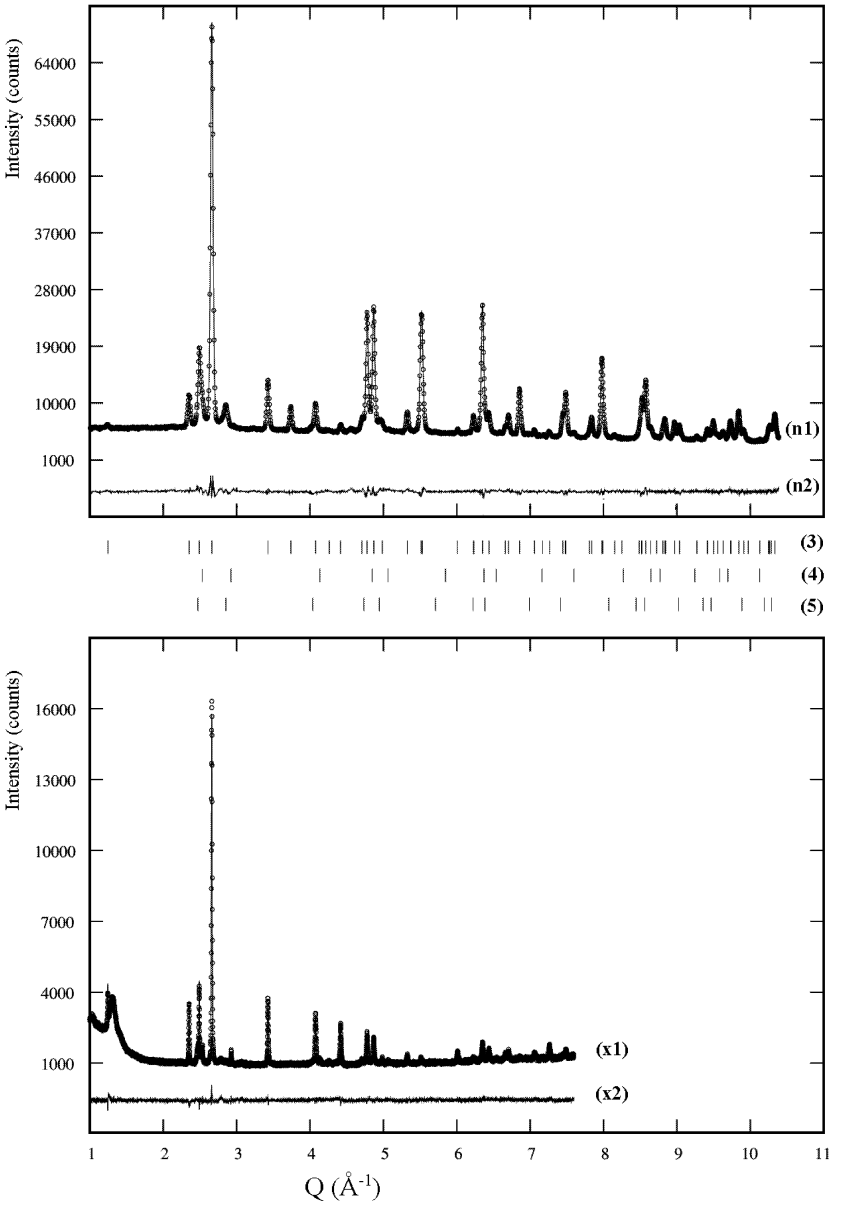

Fig. 4. Observed and calculated (n1), and difference (n2) neutron (top) and X-ray (bottom) powder diffraction patterns for SHS sample, and Bragg positions for trigonal titanium carbo-deuteride (3), cubic titanium carbo-deuteride (4) and TiD_2 (5).

of its structural disorder, but they have been seen in carbo-hydride samples as prepared by conventional synthesis [6]. As to their hydrogen storage capacities the trigonal phase has a higher hydrogen content (1.29 wt%, 57.4 g l^{-1}) than the cubic phase (1.11 wt%, 50.4 g l^{-1}). While the maximum possible hydrogen content of the trigonal phase can be estimated to be close to the composition $TiC_{0.5}H_{1.0}$ (complete filling of a subset of tetrahedral sites at fixed carbon content) that of the cubic phase cannot be easily estimated because of its variable carbon content. In fact, at carbon contents lower than that of the presently studied compound ($TiC_{0.48}D_{0.60}$) the hydrogen content could increase considerably due to the possibility of higher occupancies of octahedral and tetrahedral sites by hydrogen.

The thermal properties of the samples studied show significant differences as can be seen from the thermogravimetric (TG) and differential thermal analysis (DTA) data. As shown in Fig. 2a the CS sample shows three endothermic DTA peaks. Those at 778 and 848 K are accompanied by a significant weight loss as shown by the TG data and can be attributed to deuterium desorption from the cubic phase, while that at 1043 K is accompanied by no significant weight loss and can be attributed to desorption from binary TiD_2. The thermograms are very similar to, though shifted to higher temperatures than,

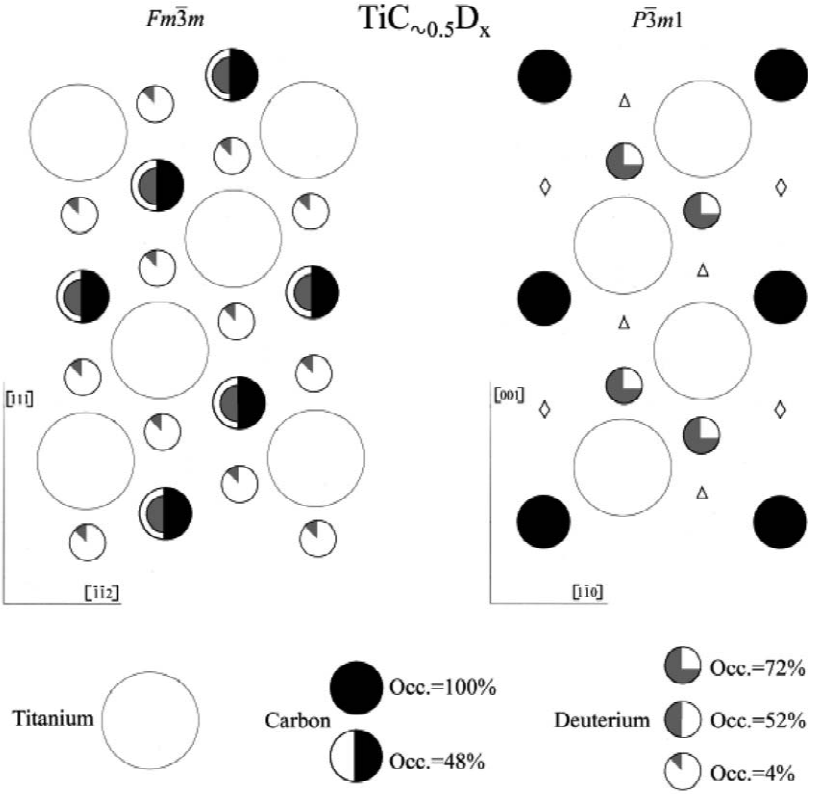

Fig. 5. Structure of titanium carbo-deuterides. Disordered cubic modification in ($1\bar{1}0$) plane (left) and partially ordered trigonal modification in (11.0) plane (right). Carbon occupies octahedral interstices in the *f.c.c.* and *h.c.p.* metal host structures, while deuterium occupies octahedral interstices in the *f.c.c.* and tetrahedral interstices in the *h.c.p.* host structure. Empty interstices in trigonal structure are indicated by lozenges (octahedral) and triangles (tetrahedral).

those reported for the cubic thorium carbo-deuteride phase that transforms irreversibly to its hexagonal analogue at 653 K [19]. However, X-ray diffraction patterns of the present sample after the experiment showed that no such transformation had occurred, just a decrease of the cubic cell parameter. On the other hand, the SHS sample shows only two endothermic peaks (see Fig. 2b) of which the smaller one at 823 K can be attributed to deuterium desorption from the cubic minority phase, and the larger one at 1093 K to desorption from the trigonal phase. Interestingly, the TG data show a constant weight loss in this temperature interval. Given that deuterium stabilises the formation of the trigonal phase and that this phase was found to be absent after the DTA and TG experiments it is possible that this weight loss is due to a gradual transformation of the trigonal to the cubic phase. Clearly, high-temperature diffraction experiments are necessary to confirm this hypothesis.

4. Conclusion

Except for details in atomic ordering the titanium carbo-deuterides obtained by combustion synthesis are structurally identical to those of titanium carbo-hydrides obtained by conventional synthesis. The thermal stability of the cubic phase is lower by more than 200 K compared to the trigonal phase and binary TiH_2. This difference is attributed to the specific atom environment of hydrogen in the metal atom host structures. In the cubic carbo-hydride phase that desorbs at lower temperature the hydrogen atoms are located mainly in large octahedral interstices and thus are likely to be more weakly bonded than the hydrogen atoms situated in small tetrahedral interstices of the trigonal carbo-hydride phase and cubic TiH_2 that desorb hydrogen at higher temperature.

Acknowledgements

This work was supported by the Swiss National Science Foundation and the Swiss Federal Office of Energy.

References

[1] H. Bittner, Mh. Chem. 95 (1964) 1514.
[2] H. Goretzki, H. Bittner, H. Nowotny, Mh. Chem. 95 (1964) 1521.

[3] J. Rexer, D.T. Peterson, Compounds of interest in nuclear reactor technology, IMD Special Rep. Ser. 10 (13) (1964) 327.
[4] K. Yvon, H. Nowotny, R. Kieffer, Mh. Chem. 98 (1967) 2164.
[5] G.W. Samsonow, W.W. Morosow, Mh. Chem. 102 (1971) 1667.
[6] I.S. Latergaus, V.T. Em, I. Karimov, D.Y. Khvatinskaya, S.K. Dolukhanyan, Inorg. Mater. 20 (10) (1984) 1420.
[7] G. Hägg, Z. Phys. Chem. B II (1931) 433.
[8] H. Goretzki, E. Ganglberger, H. Nowotny, H. Bittner, Mh. Chem. 96 (1965) 1563.
[9] R.A. Andrievskii, E.B. Boiko, V.P. Kalinin, Sov. Phys. Crystallogr. (Kristallografiya) 12 (6) (1967) 930.
[10] V.N. Bykov, V.S. Golovkin, V.P. Kalinin, V.A. Levdiky, V.I. Shcherbak, Ukrain'kii Fizichnii Zhurnal (Russian Ed.) 14 (10) (1969) 1713.
[11] S.K. Dolukhanyan, J. Alloys Comp. 253–254 (1997) 10.
[12] S.K. Dolukhanyan, V.S. Shekhtman, N.N. Aghajanyan, K.A. Abrahamyan, K.S. Harutyunyan, A.G. Aleksanyan, H.G. Hakobyan, O.P. Ter-Galstyan, J. Alloys Comp. 330–332 (2002) 551.
[13] A.G. Aleksanyan, N.N. Aghajanyan, S.K. Dolukhanyan, N.L. Mnatsakanyan, K.S. Harutyunyan, V.S. Hayrapetyan, J. Alloys Comp. 330–332 (2002) 559.
[14] P. Fischer, G. Frey, M. Koch, M. Könnecke, V. Pomjakushin, J. Schefer, R. Thut, N. Schlumpf, R. Bürge, U. Greuter, S. Bondt, E. Berruyer, Physica B 276 (2000) 146.
[15] G. Lobier, Colloq. Int. Centre Natl. Recherche Sci. (Paris) 1 (1970) 405.
[16] J. Rodriguez-Carvajal, PROGRAM FullProf.2000 Multi-Pattern (Version 1.5), Laboratoire Léon Brillouin (CEA-CNRS), France, 2000, April.
[17] P.E. Irving, C.J. Beevers, Metall. Trans. 2 (1971) 613.
[18] H. Goretzki, Phys. Status Solidi 20 (1967) K141.
[19] M. Makovec, Z. Ban, J. Less-Common Metals 21 (1970) 169.